

Research Report
Anatomy/Histology/
Embryology



NOX4 and its association with myeloperoxidase and osteopontin in regulating endochondral ossification

Kayoung Ko ^{1,†}, Seohee Choi ^{1,†}, Miri Jo ¹, Chaeyoung Kim ¹,
Napissara Boonpraman ², Jihyun Youm ³, Sun Shin Yi ^{1,4,*}

¹BK21 Four Project, Department of Medical Sciences, Soonchunhyang University, Asan 31538, Korea

²Department of Translational Neuroscience, College of Human Medicine, Michigan State University, Grand Rapids, MI 48824, USA

³Department of Gerontology, Graduate School of East-West Medical Science, Kyunghee University, Yongin 17104, Korea

⁴iConnectome Co., LTD, Cheonan 31168, Korea

 OPEN ACCESS

Received: Feb 26, 2024

Revised: Apr 28, 2024

Accepted: May 13, 2024

Published online: May 24, 2024

*Corresponding author:

Sun Shin Yi

Department of Biomedical Laboratory Science,
College of Medical Sciences, Soonchunhyang
University, 22 Soonchunhyang-ro, Sinchang-
myeon, Asan 31538, Korea.

Email: admiral96@sch.ac.kr

https://orcid.org/0000-0001-8568-0954

[†]Kayoung Ko and Seohee Choi equally
contributed to this work.

ABSTRACT

Importance: Endochondral ossification plays an important role in skeletal development. Recent studies have suggested a link between increased intracellular reactive oxygen species (ROS) and skeletal disorders. Moreover, previous studies have revealed that increasing the levels of myeloperoxidase (MPO) and osteopontin (OPN) while inhibiting NADPH oxidase 4 (NOX4) can enhance bone growth. This investigation provides further evidence by showing a direct link between NOX4 and MPO, OPN in bone function.

Objective: This study investigates NOX4, an enzyme producing hydrogen peroxide, in endochondral ossification and bone remodeling. NOX4's role in osteoblast formation and osteogenic signaling pathways is explored.

Methods: Using NOX4-deficient (NOX4^{-/-}) and ovariectomized (OVX) mice, we identify NOX4's potential mediators in bone maturation.

Results: NOX4^{-/-} mice displayed significant differences in bone mass and structure. Compared to the normal Control and OVX groups. Hematoxylin and eosin staining showed NOX4^{-/-} mice had the highest trabecular bone volume, while OVX had the lowest. Proteomic analysis revealed significantly elevated MPO and OPN levels in bone marrow-derived cells in NOX4^{-/-} mice. Immunohistochemistry confirmed increased MPO, OPN, and collagen II (COLII) near the epiphyseal plate. Collagen and chondrogenesis analysis supported enhanced bone development in NOX4^{-/-} mice.

Conclusions and Relevance: Our results emphasize NOX4's significance in bone morphology, mesenchymal stem cell proteomics, immunohistochemistry, collagen levels, and chondrogenesis. NOX4 deficiency enhances bone development and endochondral ossification, potentially through increased MPO, OPN, and COLII expression. These findings suggest therapeutic implications for skeletal disorders.

Keywords: Endochondral ossification; myeloperoxidase; NADPH oxidase 4; osteopontin; ovariectomy

© 2024 The Korean Society of Veterinary Science

This is an Open Access article distributed under the terms of the Creative Commons Attribution Non-Commercial License (<https://creativecommons.org/licenses/by-nc/4.0>) which permits unrestricted non-commercial use, distribution, and reproduction in any medium, provided the original work is properly cited.

ORCID iDs

Kayoung Ko
<https://orcid.org/0009-0004-4368-2600>
Seohee Choi
<https://orcid.org/0009-0000-9963-4377>
Miri Jo
<https://orcid.org/0009-0003-4698-2206>
Chaeyoung Kim
<https://orcid.org/0009-0001-6008-0503>
Napissara Boonpraman
<https://orcid.org/0000-0002-8244-0530>
Jihyun Youm
<https://orcid.org/0009-0003-2899-0149>
Sun Shin Yi
<https://orcid.org/0000-0001-8568-0954>

Author Contributions

Conceptualization: Yi SS; Data curation: Ko K, Choi S, Jo M, Youm J; Formal analysis: Kim C; Funding acquisition: Yi SS; Investigation: Ko K, Choi S, Jo M; Methodology: Boonpraman N; Resources: Yi SS; Supervision: Yi SS; Validation: Yi SS; Visualization: Ko KY, Choi S; Writing - original draft: Ko K; Writing - review & editing: Yi SS.

Conflict of Interest

The authors declare no conflicts of interest.

Funding

This research was supported by the National Research Foundation (NRF) NRF-2018R1D1A3B07047960, and Soonchunhyang University Research Fund.

INTRODUCTION

A myriad of signaling routes stringently regulates skeletal maturation and growth, particularly through the process of endochondral ossification. This biological mechanism is pivotal in transforming the cartilaginous model of embryonic bones into mature bone tissue, contributing to their longitudinal growth and development [1]. The chondrocytes, specialized cells in cartilage, play a critical role in this process, undergoing a series of differentiation steps that lead to the growth of long bones [2,3]. The endochondral ossification process involves two major cell types, osteoblasts, and osteoclasts, with the epiphyseal plate in long bones being crucial for proper growth [1].

Recent research has indicated a potential link between skeletal diseases like osteoporosis and osteoarthritis and elevated levels of intracellular reactive oxygen species (ROS) [4-8]. These ROS, generated through various pathways, can disrupt the balance between prooxidants and antioxidants, leading to oxidative stress [9]. This stress is associated with tissue inflammation, aging, and degeneration and is increasingly being linked to bone biology and redox balance regulation [10]. The NOX family, particularly NADPH oxidase 4 (NOX4), is a predominant contributor to intracellular ROS production [11]. NOX4 is unique in the NOX family for its constant activity and predominant hydrogen peroxide production [12]. It differentiates many cell types and is particularly significant in bone modeling. The ongoing ROS production by NOX4 is suggested to be linked to skeletal pathologies. Modulating NOX4 levels could potentially reduce ROS concentrations and improve bone solidity [13-16]. Furthermore, NOX4 expression levels have been reported to influence bone conditions and regulate activities in the intercellular system, including the endochondral ossification process [17]. Although the impact of NOX4 on bone equilibrium is clear, comprehensive studies are needed to fully understand its role in endochondral ossification. The paper's premise suggests a correlation between the progression of the epiphyseal plate and NOX4 expression levels. It hypothesizes that NOX4 expression might modulate endochondral ossification through certain intermediary agents. To explore this hypothesis, animal models, specifically NOX4-deficient (NOX4^{-/-}) mice and ovariectomized (OVX) mice, were employed.

This research aims to deepen the understanding of NOX4's role in bone health, potentially contributing to the development of treatments for skeletal diseases linked to ROS and oxidative stress.

METHODS**Experimental animals**

C57BL/6J wild-type mice (n = 11; 16 weeks old female, 23 ± 1 g) and NOX4 knock out (KO) mice (n = 8; 16 weeks old female, 23 ± 1 g) from the Jackson Laboratory (Jackson Laboratory, USA) were used for the experiments. Mice were raised at constant temperature (22°C ± 2°C) and humidity (60%) under a 12-h light/12-h dark cycle (light cycle:dark cycle from 07:00 to 19:00). All the mice were provided with available food (2018S; Harlan, USA) and distilled water (DW). The experimental protocol of this study (SCH23-0028) was approved by the Institutional Animal Care and Use Committee (IACUC) of Soonchunhyang University.

Ovariectomy

Bilateral OVX was performed under 0.5% isoflurane inhalation (Hana Pharm, Korea) anesthesia in all OVX groups by removing both ovaries from the abdominal cavity. Control operation (ovary identification) was performed for mice in Control groups. After 8 weeks following OVX, blood was collected from the abdominal vein to confirm the success of OVX of the animals by estradiol test before sacrificing the animals.

Tissue preparation

All mice were euthanized at the same age. The animals were cardially perfused with 4% paraformaldehyde (PFA; Sigma-Aldrich, USA). The left side of the femur and tibia of each mouse was removed and post-fixed 4% PFA for 24 h in a refrigerated state. The tissues were decalcified for 3 days in a RapidCal Immuno (BBC Biochemical, USA). The fresh solution was used each day. Each bone sample was embedded in paraffin and sectioned to the thickness of 5- μ m.

Proteome arrays

Bone marrow protein lysates sourced from both control and NOX4 KO groups were utilized for the Proteome Profiler Mouse XL Cytokine Array (R&D Systems, USA) to analyze 111 soluble proteins, which comprised cytokines, chemokines, and growth factors. Nitrocellulose membranes, each containing 111 distinct capture antibodies printed in duplicate, were utilized to incubate the protein lysate samples overnight at 4°C. The detection antibody, being a cocktail of biotinylated antibodies, was then used to incubate the membranes for 2 h at room temperature, followed by incubation with streptavidin conjugated to horseradish-peroxidase (HRP) for 30 min at room temperature. Immunoreactive spots were detected on the membranes using Chemi Reagent Mix and exposed to X-ray film for 1–10 min. The results obtained were analyzed using image software (HLImage⁺⁺ Version 25.0.Or, <https://www.wvision.com/QuickSpots.html>; Western Vision Software, USA).

Staining for histomorphometry

Hematoxylin and eosin (H&E) staining

Using Harris hematoxylin (BBC Biochemical) and Eosin Y (pH 4.65; BBC Biochemical) dye, we stained the bone tissue embedded in paraffin using the general degenerative H&E staining method. For this purpose, the tissue was differentiated the hyperstained hematoxylin staining with 1% acid alcohol and blued using 1% ammonium water. After dehydration of 70%–100% alcohol, it is sealed with Eukitt Quick-hardening mounting medium (Sigma-Aldrich). Histomorphometry was used to analyze bone mass, structure, and resorption in a specific area of the femur, while cortical bone thickness was measured in another region.

Masson's trichrome staining

Masson trichrome stain is the most widely used staining method for collagenic fiber dyeing and Masson Trichrome kit (PolyScience, USA) was used. The bone tissue is hydrated. After washing in running water, perform secondary fixation for 1 h in Bouin solution with picric acid heated to 50°C. After removing picric acid through 50%–70% alcohol each for 5 min, nuclear dyeing is performed in Weigert iron hematoxylin, which is blocked from light, for 5 min. Dye the cytoplasm and muscle fiber in a Biebrich scarlet-acid fuchsin solution. Separate large collagenic fibers in a phosphomolybdic phosphotungstic acid solution for 5 min and dye them in a light-blocked aniline blue solution heated to 40°C for 5 min. After differentiating with 1% acetic acid, dehydration was performed using ascending series ethanol (70% to 100%) and then air dried for 30 min. Afterward, it is sealed with Eukitt Quick-hardening mounting medium (Sigma-Aldrich).

Safranin O-fast green staining

Safranin O-fast green staining is an experiment to compare the growth and differentiation degree of joint cartilage. Use the NovaUltra Safranin O Stain Kit (IHCWORLD, USA). The bone tissue is hydrated and dye it Weigert iron hematoxylin for 3 min and wash it in running water for 5 min. Dye at 0.005% fast green for 5 min and separate for 30 sec in 1% acetic acid. Dye it in 1% Safranin O solution for 5 min and wash it with DW, then the tissue slides and dehydrate with in 95%–100% alcohol and air dried for 30 min. The prepared tissue slides were coverslipped with Eukitt Quick-hardening mounting medium (Sigma-Aldrich).

Toluidine blue staining

To determine the ossification of tissue epiphyseal plates, Toluidine blue staining was performed using a Toluidine Blue Stain Kit (IHCWORLD). Basically, the staining followed the manufacturer's direction of the kit. Briefly, the bone tissue is hydrated and dyed with 1% Toluidine blue solution. Dyeing can be checked with a microscope. After that, it is washed three times with DW and dehydrated through 95% and 100% ethanol two times quickly. The slides were entirely dried in the air for 30 min, and then the prepared tissue slides were coverslipped with Eukitt Quick-hardening mounting medium (Sigma-Aldrich).

Plasma estradiol level measurement

To verify the accomplishment of OVX, plasma estradiol levels were measured using a mouse/rat estradiol ELISA kit (Calbiotech, USA) according to the manufacturer's instructions. Briefly, the samples, estradiol (E2) standards, and controls in goat anti-rabbit immunoglobulin G (IgG)-coated 96-wells were incubated with estradiol-HRP conjugate reagent and rabbit-estradiol reagent at room temperature for 90 min. An established amount of HRP-labeled E2 was used to compete with the endogenous E2 in samples, standard, or quality control plasma for a fixed number of binding sites of the specific E2 antibody during the incubation. Unbound E2 peroxidase conjugate was removed, and then wells were washed. Next, a solution of TMB Reagent was added and incubated at room temperature for 20 min for color development. The color development was then stopped with the addition of stop solution, and the absorbance was measured spectrophotometrically at 450 nm. After sacrificing the OVX-animals, data from animals that did not show significantly low estradiol levels were excluded from statistical analysis.

Immunohistochemistry for myeloperoxidase (MPO), osteopontin (OPN), and collagen II (COLII)

The bone tissue cut to 5- μ m is deparaffinized, hydrated, and sequentially treated with 0.3% hydrogen peroxide in phosphate-buffered saline (PBS) for 15 min. After washing with PBS 3 times, CAS-Block Histochemical Reagent (Invitrogen, USA) blocks non-specific reactions. Polyclonal rabbit anti-osteopontin (1:200; Proteintech, USA), polyclonal rabbit anti-myeloperoxidase (1:200; Dako, Denmark), polyclonal rabbit anti-collagen II (1:100; Abcam, UK) was used as the primary antibody and stored in a wet state at 4°C for 18 h. The secondary antibody is reacted at room temperature for 2 h using a biotinylated anti-rabbit (Vector Laboratories, USA). React for 30 min using the VECTASTAIN Elite ABC kit Peroxidase (Standard; Vector Laboratories) and color it with 3,3-diaminobenzidine tetrahydrochloride (DAB; Sigma-Aldrich).

Western blot

Proteins from C57BL/6J, OVX, and NOX4 KO mice were subjected to lysis in RIPA buffer (Sigma-Aldrich) containing phosphatase inhibitor (GenDEPOT, USA). The protein

concentration was ascertained using the bovine serum albumin (BSA) standard. After quantification, equivalent quantities of protein samples were loaded onto each lane with 10% Tris-glycine and transferred to PVDF membranes (Bio-Rad, USA). Subsequently, the membrane was blocked with 1X TBST (10X TBS with Tween 20; Biosesang, Korea) supplemented with 5% BSA. The membranes were subjected to incubation with polyclonal rabbit anti-OPN (1:100 dilution; R&D Systems), rabbit anti-MPO (1:1,000 dilution; Dako), rabbit anti-collagen II (1:50; Abcam, UK) and polyclonal rabbit anti-GAPDH (1:10,000 dilution; Cell Signaling, USA) at 4°C overnight. These membranes were then incubated with HRP-conjugated goat anti-rabbit IgG (1:2,000; Vector Laboratories) for 2 h at room temperature. Immunoreactive bands were visualized with a SuperSignal West Pico Chemiluminescent Substrate (Thermo Scientific, USA).

Statistics

To ensure objectivity, all measurements were performed under blinded conditions by two observers per experiment under identical conditions. All slide images were scanned with Ultra-high resolution image capture through MoticEasyScan One Slide Scanner (Motic, China) Stained bone sections were quantified with ImageJ software v1.52a (National Institutes of Health, USA). The data shown represents the experimental mean \pm SD for each experimental group. Ordinary one-way analysis of variance calculated statistical significance and multiple comparison tests using Turkey's Method. The p values < 0.05 were considered statistically significant.

RESULTS

Estradiol levels

The confirmation of the successful OVX surgery was assessed by measuring the estradiol levels in the animals' blood. The results showed that the OVX group had significantly reduced estradiol levels compared to the Control and NOX4^{-/-} mice (**Fig. 1**).

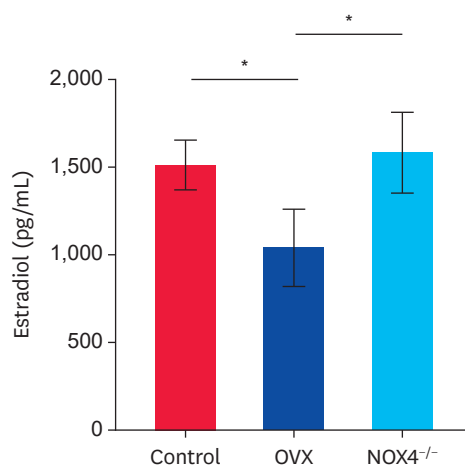


Fig. 1. Evaluation of serum E2 levels in each group after OVX. It was confirmed that the proportion of E2 is significantly reduced in the OVX group compared to the non-surgical group. Error bars represent mean \pm SD ($n = 3$ per each group). E2, estradiol; OVX, ovariectomy; NOX4^{-/-}, NADPH oxidase 4-deficient. * $p < 0.05$.

Phenotypic analysis by the bone morphological features in the femur typically observed in NOX4^{-/-} mice

The findings are derived from comparing bone mass and structure among the Control, OVX, and NOX4^{-/-} groups, as visualized through H&E staining (Fig. 2A). Comparative analysis of trabecular bone volume revealed that the NOX4^{-/-} group had the most pronounced volume. In contrast, the OVX group displayed a notably diminished volume relative to the Control group. Histomorphometric evaluations encompassing parameters such as trabecular bone volume (BV/TV), trabecular bone number (Tb.N), trabecular bone length (Tb.Le), trabecular bone thickness (Tb.Th), and cortical bone thickness (Ct.Th) were undertaken (Fig. 2B, Table 1). Among the groups, the NOX4^{-/-} group consistently exhibited the highest values for these parameters. Conversely, the OVX group displayed the lowest values in comparison to the Control group.

Femoral bone marrow-derived MSC proteomic profiling present in the thighbone of experimental animals

To closely investigate the role of the NOX4 gene in contributing to osteogenic potential, we conducted a proteome array analysis on bone marrow mesenchymal stem cells (MSCs)

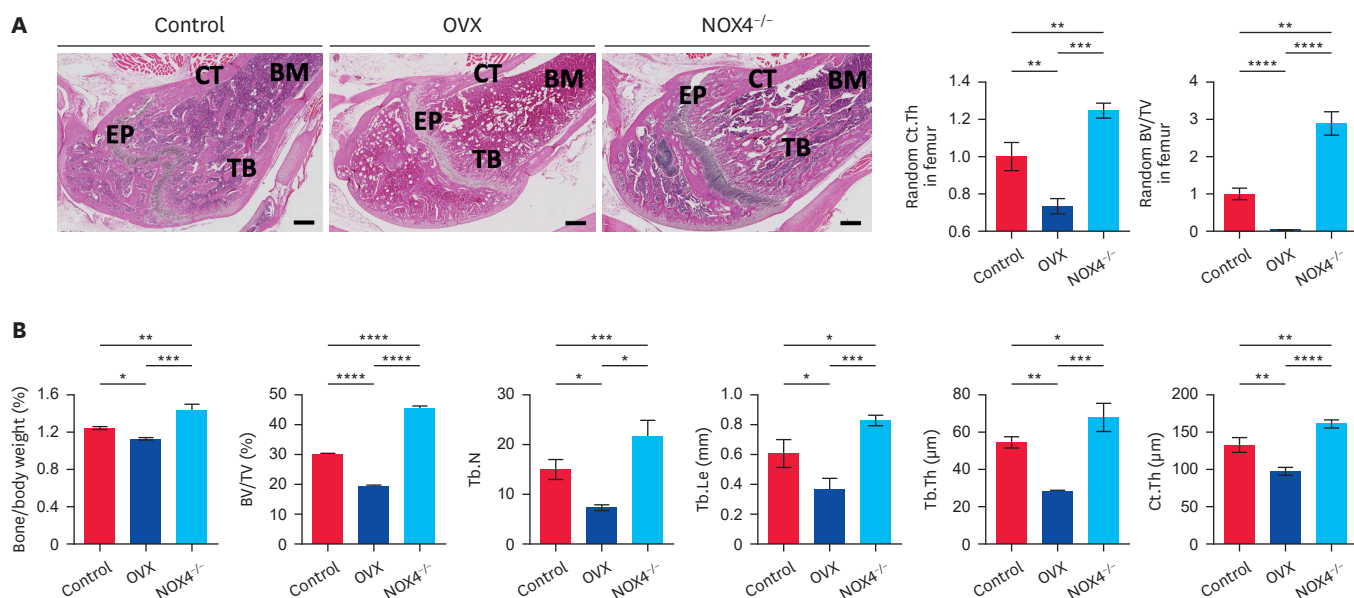


Fig. 2. H&E staining of the animals’ femurs and histomorphometry of the femurs in the mice. (A) The cortical bone thickness and trabecular volumes were significantly higher in NOX4^{-/-} groups compared to those in both Control and OVX groups. (B) Femur histomorphometry measurements in each group. Ordinary one-way analysis of variance calculated statistical significance and multiple comparison tests using Turkey’s Method. Error bars represent mean ± SD (n = 3 per each group). Scale bar = 300 µm.

H&E, hematoxylin and eosin; NOX4^{-/-}, NADPH oxidase 4-deficient; OVX, ovariectomy; BM, bone marrow; CT, cortical bone; EP, epiphyseal plate; TB, trabecular bone; BV/TV, trabecular bone volume (%); Tb.N, trabecular bone number (N/epiphyseal); Tb.Le, trabecular bone length (longitudinal thickness; mm); Tb.Th, trabecular bone thickness (cross thickness; µm); Ct.Th, cortical bone thickness.
*p < 0.05; **p < 0.01; ***p < 0.001; ****p < 0.0001.

Table 1. Femur histomorphometry measurements in each group

Groups	Bone mass & bone structure				
	BV/TV (%)	Tb.N (number)	Tb.Le (mm)	Tb.Th (µm)	Ct.Th (µm)
Control	30.06 ± 0.33	14.25 ± 2.22	0.59 ± 0.09	54.06 ± 3.04	132.67 ± 10.03
OVX	19.36 ± 0.39****	7.33 ± 0.58*	0.37 ± 0.07*	28.55 ± 0.27**	97.23 ± 5.43**
NOX4 ^{-/-}	45.35 ± 0.35****, #####	20 ± 4.08***, #	0.81 ± 0.16*, ###	68.03 ± 7.50*, ###	165.24 ± 5.39**, #####

OVX, ovariectomy; NOX4^{-/-}, NADPH oxidase 4-deficient; TB, trabecular bone; BV/TV, trabecular bone volume; Tb.N, trabecular bone number (N/epiphyseal); Tb.Le, trabecular bone length (longitudinal thickness; mm); Tb.Th, trabecular bone thickness (cross thickness; µm); Ct.Th, cortical bone thickness.

*p < 0.05; **p < 0.01; ***p < 0.001; ****p < 0.0001 vs. Control, #p < 0.05; ###p < 0.001; #####p < 0.0001 vs. OVX. Ordinary one-way analysis of variance calculated statistical significance and multiple comparison tests using Turkey’s Method (n = 3 per each group).

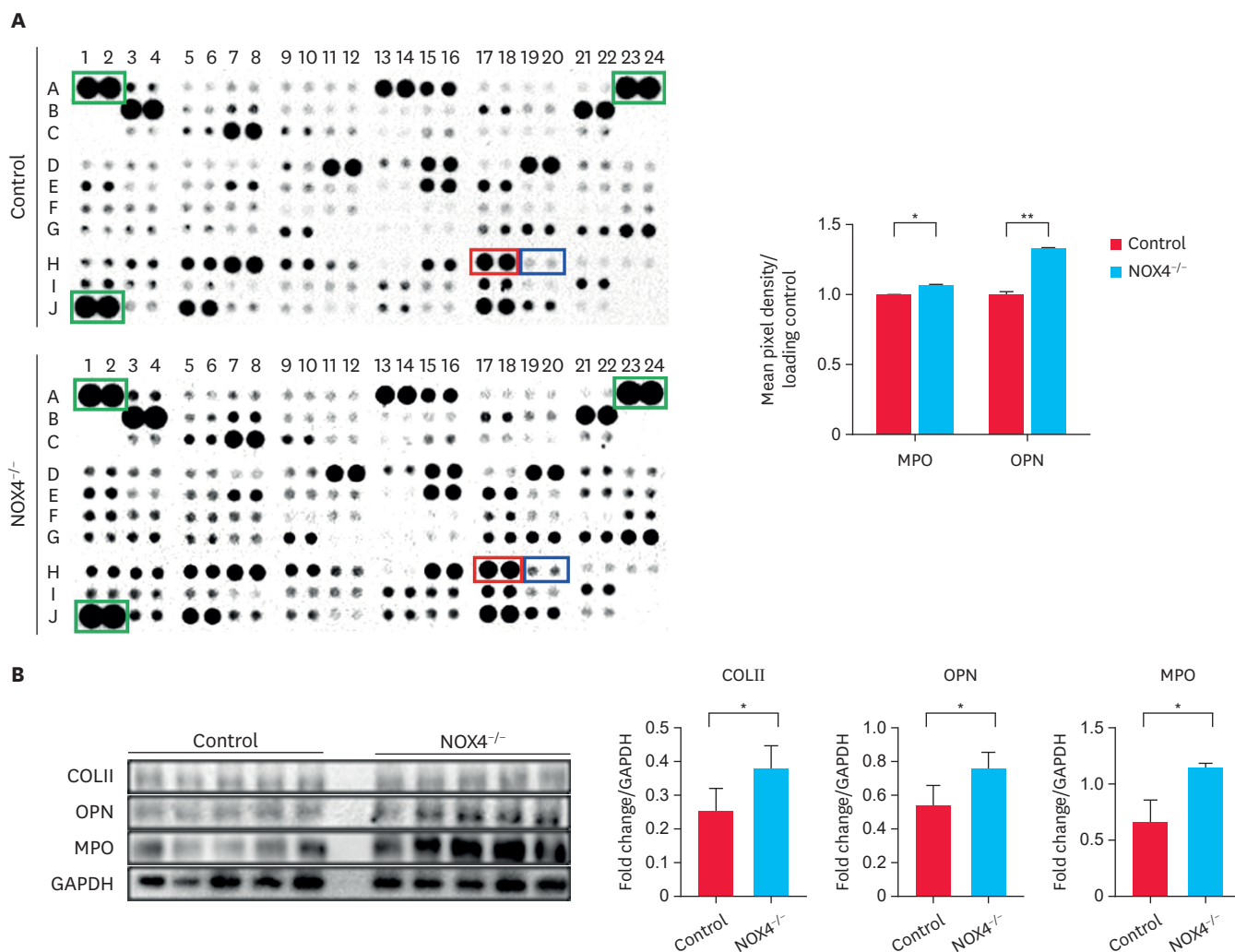


Fig. 3. MPO and OPN are predominantly elevated in femoral MSCs. (A) Representative images and quantification of the proteome profiler murine XL cytokines array immunoblot analysis of 111 diverse cytokines, chemokines, growth factors, or extracellular signaling molecules of the mesenchymal cells of NOX4^{-/-} group. (B) Protein expression of COLII, OPN, and MPO was significantly increased in the extracted mesenchymal cells in the bone marrow of NOX4^{-/-} mice. The red-lined boxes are MPOs, the blue-lined boxes are OPNs, and the green-lined boxes on both ends of the three membranes are reference genes. MPO, myeloperoxidase; OPN, osteopontin; MSC, mesenchymal stem cell; NOX4^{-/-}, NADPH oxidase 4-deficient; COLII, collagen II; GAPDH, glyceraldehyde 3-phosphate dehydrogenase.

Error bar represented mean \pm SD (Control group n = 5; NOX4^{-/-} group n = 5).

* $p < 0.05$; ** $p < 0.01$ vs. Control.

extracted from the femur (**Fig. 3A**). Notably, in the NOX4^{-/-} group, MPO and OPN levels were significantly elevated compared to those observed in the Control group (**Fig. 3A**). After the proteome array observation, the disparities discerned between the Control and NOX4^{-/-} groups further substantiated the analysis of variations in the expression of MPO, OPN, and COLII, as assessed by western blot (**Fig. 3B**). The expression levels of MPO, OPN, and COLII were markedly higher in the MSCs derived from the NOX4^{-/-} group than in those from the Control group.

Immunohistochemistry for MPO, OPN, and COLII expression

Immunohistochemistry (IHC) was executed to identify the expression sites and characteristics of MPO, OPN, and COLII near the femoral epiphyseal plate of the animals across the different groups. Significantly elevated positive signals for MPO, OPN, and COLII

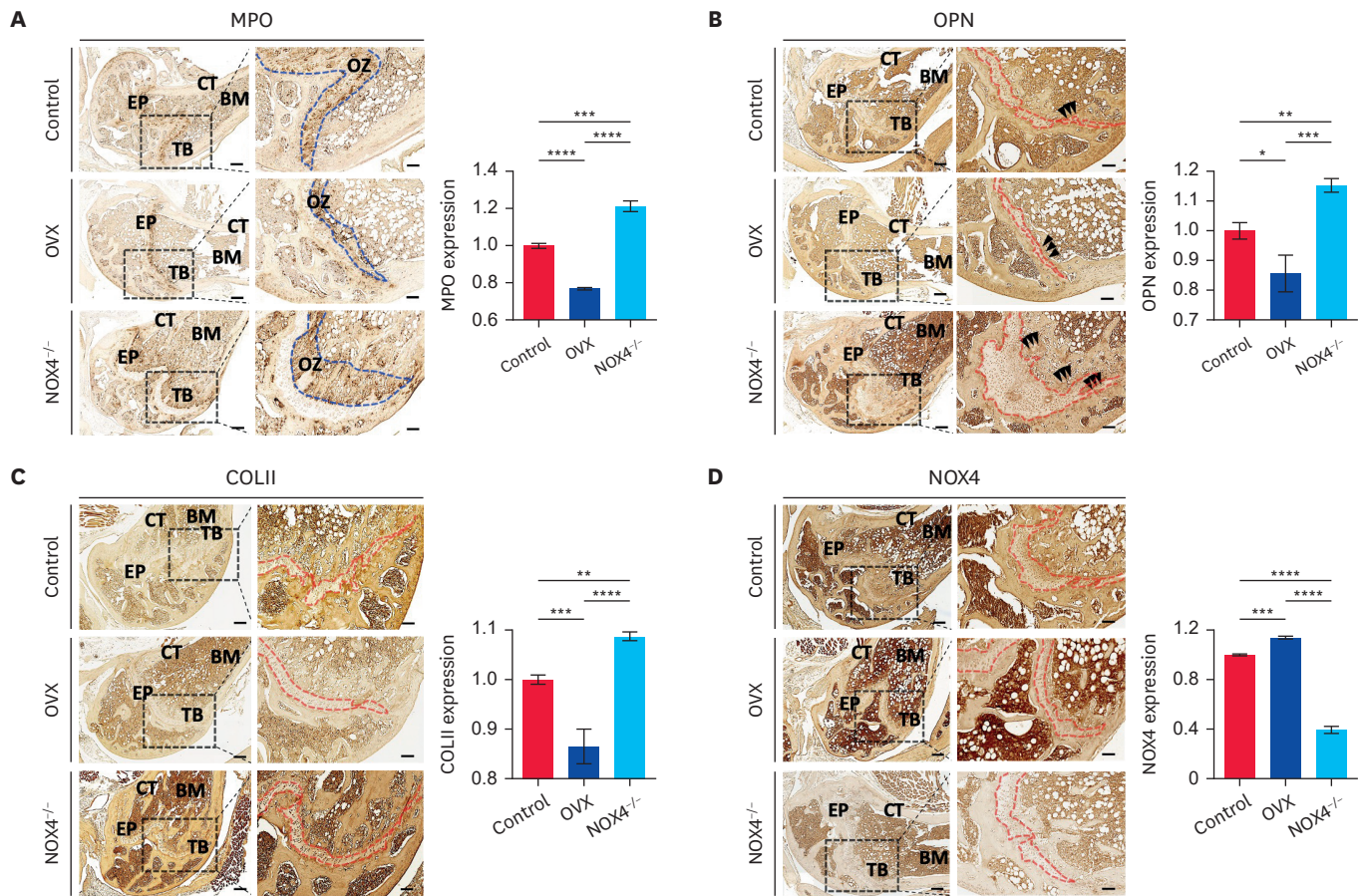


Fig. 4. Immunohistochemistry to observe MPO, OPN, COLII, and NOX4 expression around the epiphyseal plates. (A) MPO around the epiphyseal plate is well expressed in NOX4^{-/-} mice but not in OVX mice. (B) OPN in NOX4^{-/-} is highly expressed in the epiphyseal plates; however, significantly downregulated in the OVX mice. (C) COLII is highly expressed in the chondrocyte layer in NOX4^{-/-} mice. (D) NOX4 expression is elevated in the chondrocyte layer in OVX mice compared to control mice. The inset images in the right corner of each picture mean a black dotted square; the blue dotted circles stand for the ossification zone; the red dotted circles stand for the epiphyseal plate.

Ordinary one-way analysis of variance calculated statistical significance and multiple comparison tests using Turkey's Method. The arrowheads indicate OPN-expressed points. Error bars represent mean ± SD (n = 3 per each group). Scale bar = 300 µm and 100 µm (at the magnified images).

MPO, myeloperoxidase; OPN, osteopontin; COLII, collagen II; NOX4, NADPH oxidase 4; NOX4^{-/-}, NADPH oxidase 4-deficient; OVX, ovariectomy; BM, bone marrow cells; CT, cortical bone; EP, epiphyseal plate; OZ, ossification zone; TB, trabecular bone.

p* < 0.05; *p* < 0.01; ****p* < 0.001; *****p* < 0.0001.

were observed around the epiphyseal plate in NOX4^{-/-} animals in all groups. However, in OVX animals, a significant decrease in the expression of these three factors was noted compared to the other groups. Upon closer examination of the figure's magnified views, high expression of these three factors was evident in the region just below the hypertrophic zone of the epiphyseal plate, where the metaphyseal bone begins (**Fig. 4A-C**). These results suggested that NOX4 deficiency leads to active participation of bone marrow cells' MSC in endochondral ossification at both the hypertrophic zone and the metaphyseal bone, potentially facilitated by MPO and OPN. In NOX4^{-/-} mice, COLII expression was notably stronger compared to the Control and OVX groups (**Fig. 4C**). Furthermore, the almost absent expression of NOX4 in NOX4^{-/-} animals was confirmed (**Fig. 4D**). Notably, in the OVX group, a significant increase in NOX4 expression was observed compared to the Control group (**Fig. 4D**).

Collagen amount and chondrogenesis in the femur

The amount of collagen expression and chondrogenesis in the epiphyseal plate of the femur was compared among the animals in each group (Fig. 5). When compared using Masson's trichrome staining, it is readily apparent that the area occupied by cortical and trabecular bones is significantly increased in the NOX4^{-/-} group. Additionally, there is a clear alteration in the area occupied by the epiphyseal plate (Fig. 5A). When staining for Safranin O-fast green and Toluidine blue in chondrocytes and comparing the epiphyseal plate

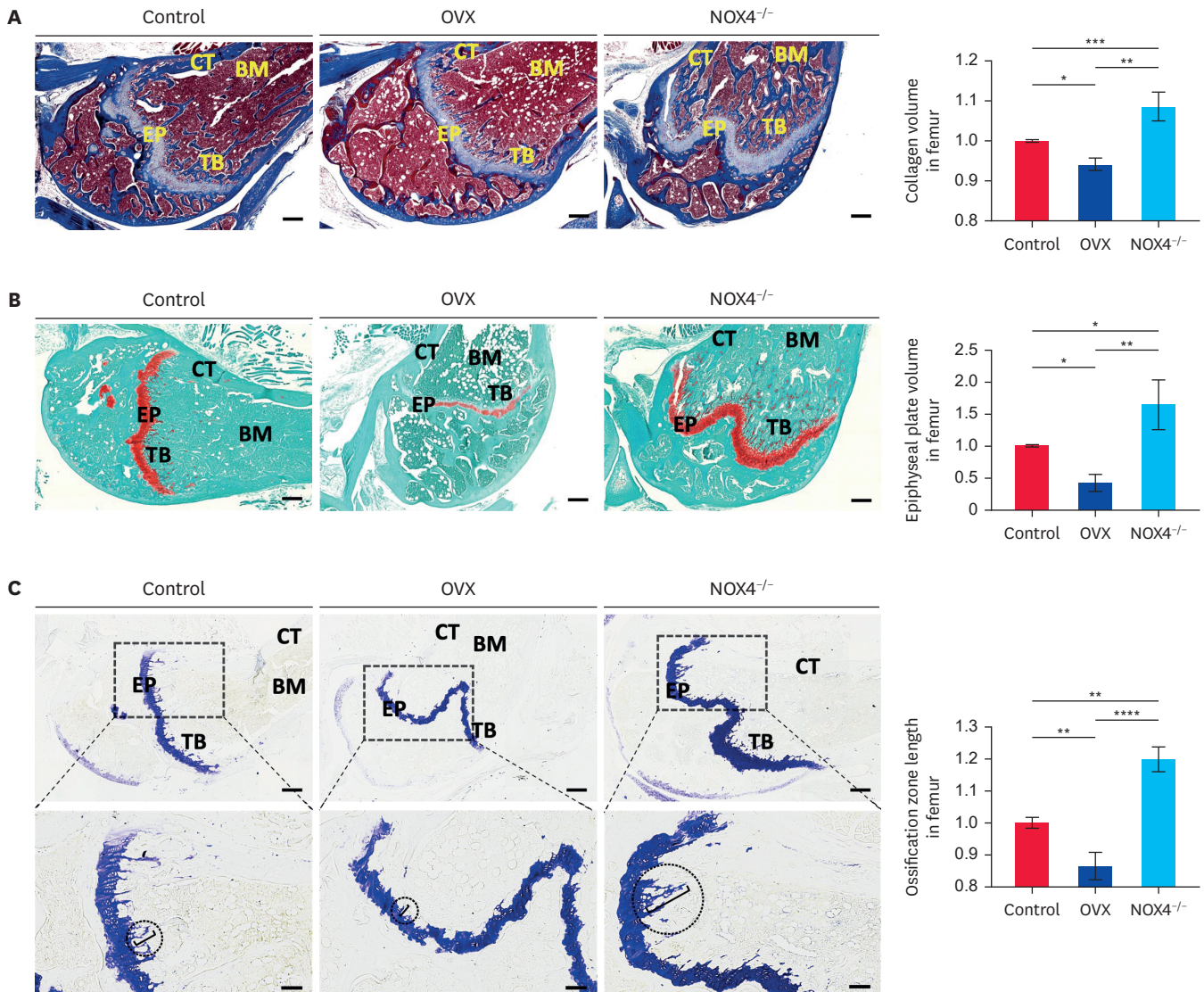


Fig. 5. Investigation of bone regeneration and epiphyseal volume changes in the femur with histological staining. (A) Masson's trichrome staining showed a large amount of collagen in NOX4^{-/-} mice and decreased collagen content in OVX mice compared to the control group. Differences in the density and thickness of cortical and trabecular bones and differences in the thickness of the epiphyseal plate are observed by the group, (B) demonstrates aggrecan, type II collagen, and glycosaminoglycans components in the joints of the epiphyseal plate and femur head stained by Safranin O, (C) demonstrates acid proteoglycan, chondrogenic components in the joints of the epiphyseal plate and femur head stained by Toluidine blue staining. It was confirmed that the NOX4^{-/-} group showed a very wide range of red and blue staining in Safranin O and Toluidine blue staining, especially in the ossification zone of the epiphyseal plates, compared to other groups. The images in the black dotted rectangles were magnified below the original histological view. The ossification widths in the black dotted circle were measured and expressed by the bar graph at the right corner of the images.

Ordinary one-way analysis of variance calculated statistical significance and multiple comparison tests using Turkey's Method. Error bars represent mean \pm SD ($n = 3$ per each group). Scale bar = 300 μ m, and 100 μ m (at the magnified images in C).

NOX4^{-/-}, NADPH oxidase 4-deficient; OVX, ovariectomy; BM, bone marrow cells; CT, cortical bone; EP, epiphyseal plate; TB, trabecular bone.

* $p < 0.05$; ** $p < 0.01$; *** $p < 0.005$; **** $p < 0.0001$.

area among different groups, a notable increase in staining intensity was observed in the NOX4^{-/-} group (**Fig. 5B and C**). Moreover, this staining was evident in the epiphyseal plate and the ossification area where metaphysis begins. The results of the OVX group exhibited significantly lower staining intensity compared to both the Control and NOX4^{-/-} groups. This suggests a marked deficiency in endochondral ossification activity. These findings align closely with the IHC results depicted in **Fig. 4**.

DISCUSSION

The vertebrate skeletal system has evolved into a dynamic and multifunctional structure, serving a range of vital roles such as safeguarding internal organs, providing attachment sites for locomotor muscles, acting as a mineral reservoir, and functioning as a hematopoietic niche [18-20]. The regulation of this complex system involves numerous signalling pathways that oversee the development, growth, and maturation of skeletal structures, spanning from early embryonic stages to adulthood [21,22]. Dysregulation of these pathways can result in various skeletal diseases in humans.

The formation of the vertebrate bony skeleton involves two distinct processes. Most craniofacial bones are formed through a process known as intramembranous ossification [23]. In this process, mesenchymal condensations directly differentiate into osteoblasts, which are responsible for bone formation. On the other hand, all other bones in the vertebrate body are created through endochondral ossification. This process begins with forming cartilage templates, which serve as the initial scaffold for bone development [24]. This process initiates with the formation of cartilage templates, serving as the initial scaffold for bone development and gradually transitioning into bone tissue over time [18-20]. Particularly, it is widely recognized that significant longitudinal bone growth significantly influences the growth rate of young animals and plays a crucial role in maintaining bone homeostasis [25]. The bone formation processes and mechanisms still raise questions, and it is necessary to piece together the components for interpretation.

Previous research has already established that NOX4^{-/-} mice exhibit increased bone density and a reduced number of osteoclasts (OCs) [14,15]. Particularly, Chen et al. [13] delve deeply into the role of NOX4 expression in the bone development of mice during their early life stages. NOX4 is one of the enzymes responsible for generating ROS within cells. The study highlights the necessity of NOX4 expression in osteo-progenitors for the differentiation, proliferation, and maturation of osteoblasts, the primary cells responsible for forming bone. The activities of these cells directly impact the health and development of bones. Focusing specifically on the regulation of bone development in the early stages of life, the research sheds light on the mechanisms by which NOX4 and ROS signaling pathways control the physiological functions of osteoblasts. This process is crucial for healthy bone growth and maintenance and could provide vital information for preventing and treating bone-related conditions like osteoporosis. The findings suggest that regulating the function of osteoblasts through NOX4 could promote bone development or reduce the risk of certain bone diseases. This underscores the potential role of NOX4 regulation in maintaining bone health and preventing bone loss. Furthermore, the study suggests therapeutic interventions targeting molecules like NOX4 could offer new methods for improving bone health and managing related diseases. Therefore, the study emphasizes the importance of NOX4 in the bone development of mice during early life stages, opening the possibility that these findings

could lead to new treatments for bone development disorders. Understanding how NOX4 and ROS regulation affect osteoblast activity and bone health is expected to contribute significantly to preventing and treating bone diseases. This investigation is profoundly fascinating because it demonstrates that our research outcomes do not contradict or conflict with existing studies, but rather, they complement them. The findings obtained by Chen et al. [13], similar to ours, accentuate the critical influence of NOX4 alongside ROS agents in bone formation. Notably, our results shed light on the nuances of endochondral ossification that have yet to be previously articulated by other studies. The enhancement of MPO or OPN expression, evidenced in NOX4 KO mice, provides compelling evidence that their expression may be contingent upon NOX4 activity. This underscores a crucial discovery, indicating that NOX4's influence extends beyond osteoblastogenesis and impacts chondrogenesis within the epiphyseal plate, marking it as an incontrovertibly significant finding. Furthermore, it is well-documented that the production of ROS in OCs depends on NADPH oxidase activity, directly impacting osteoclast formation [5]. In addition, MPO and OPN are also known to play a role in strengthening osteoclast adhesion and promoting osteoclast differentiation, migration, and activation, however, we believe that our results complement and extend the current understanding of OC function rather than challenge the validity of prior research. In the intricate process of endochondral ossification, therefore, which bears out the formation of new bone tissue, our study focuses on the pivotal roles of osteoblasts and MSCs. These cells are at the heart of bone formation, with MSCs differentiating into chondrocytes to create a cartilage template, which is the precursor to bone tissue. This cartilage then serves as a scaffold that, through the differentiation of osteoblasts, transitions into bone, highlighting the essential role of MSCs in skeletal development. Given this framework, our research investigates NOX4, MPO, and OPN expression levels in MSCs and osteoblasts explicitly. This focus aims to unearth the nuanced relationship between these biomolecules and the endochondral ossification process. Consequently, we hypothesized that NOX4 would play a significant role in bone formation in genetically deficient animals. Additionally, we postulated that chondroblast and osteoblast progenitor cells (MSCs) would display distinctive profiles of inflammatory mediators in comparison to those in normal animals. Since the OVX we performed significantly reduced the Estradiol level compared to other groups, the chronic state of Estrogen caused by OVX was believed to be well maintained (**Fig. 1**). However, according to Chen et al. [26], it also provides important insight into the relationship between the presence or absence of estrogen and the expression of NOX4. They explored how estrogen deficiency and aging contribute to bone loss through increased oxidative stress, focusing on the role of NOX4. Utilizing mice models with and without the Nox4 gene, undergoing OVX to mimic estrogen deficiency, the research found that estrogen (E2) treatment could reverse OVX-induced bone loss and senescence signaling in osteoblasts, independent of NOX4 expression. Surprisingly, NOX4 KO mice also exhibited bone loss and osteoblast senescence, suggesting that NOX4's role in these processes may be dispensable. This indicates that other mechanisms might compensate for the lack of NOX4, highlighting the complexity of bone loss and senescence pathways. For a comprehensive understanding, the full study details are available. This study suggests that bone formation outcomes induced by NOX4 in OVX animals, when treated with estrogen, do not necessarily have to be regulated by NOX4 expression [26]. Similar to the research group's findings, our observations confirmed that NOX4 expression is influenced by OVX, but estrogen treatment can facilitate bone formation through alternative signaling systems independent of NOX4 stimulation. While we observed increased expression of MPO and OPN in NOX4 KO, suggesting a close association between NOX4 and these markers, it's conceivable that estrogen could stimulate MPO and OPN independently of NOX4. However, this hypothesis requires further verification. Our results

confirmed a significant increase in bone density in NOX4^{-/-} mice compared to other groups (**Fig. 2**). Furthermore, we have identified a high correlation between NOX4 and MPO as well as OPN, a finding not previously reported by other researchers (**Fig. 3**). In other words, there have been research reports suggesting that the NOX4 deficiency [4,5], overexpression of MPO [27], and OPN [28] may each be associated with increased bone formation. However, no reports have indicated that changes in MPO and OPN expressions can be dependent on the levels of the expression of NOX4 in bone marrow-derived cells. The involvement of OPN in bone formation is not particularly surprising [29,30]; however, the potential dependence of MPO on the expression of NOX4 is a highly intriguing fact. Generally, various types of tissue damage, along with bacterial clearance by white blood cells, have been reported to be associated with MPO-derived oxidants [31]. These oxidants are linked to several major chronic conditions, including rheumatoid arthritis, cardiovascular diseases, liver diseases, diabetes, and cancer [31]. Furthermore, in line with our recently published research, MPO has been identified as a crucial key factor in developing Parkinson's disease [32]. Hence, elevated MPO activity levels may be considered a premier diagnostic tool for common inflammation-related diseases and oxidative stress biomarkers.

In the context of longitudinal growth, observing the localization of MPO and OPN expressed in the epiphysis of NOX4^{-/-} mice and the Control and OVX groups' animals is essential. As evident in the IHC images, the expression of MPO and OPN is prominently stronger in the hypertrophic area in the epiphysis and the underlying metaphysis region of NOX4^{-/-} mice compared to the other groups (**Fig. 4**). In particular, the expression of MPO and OPN in the OVX group appears to be relatively weaker, and their responsiveness to NOX4 is also high. This suggests a very strong correlation between NOX4 and MPO or NOX4 and OPN. For these reasons, it was observed that the thickness of the epiphyseal plate in the femur of NOX4^{-/-} mice was the greatest, while animals in the OVX group exhibited lower results than the Control group (**Fig. 5**). Numerous studies have demonstrated the essential role of ROS in immune cells, and slight increases in ROS levels are known to activate signaling pathways that correspond to normal aging [33-35]. The arrival of immune cells at sites of bone injury marks a pivotal step in fracture healing, with enzymes such as MPO and eosinophil peroxidase (EPO), secreted by these cells playing a significant role in defending against bacterial threats through oxidative mechanisms [36]. Beyond this, several investigations reveal that peroxidase enzymes also actively encourage osteoblastic cells to produce collagen I and form a mineralized extracellular matrix, a process vital for bone repair and regeneration [36-38]. This stimulation of collagen production occurs post-translationally, driven by prolyl hydroxylase but notably without the need for ascorbic acid, suggesting a novel pathway of bone matrix formation [36]. Furthermore, osteoblasts quickly incorporate MPO and EPO, using their enzymatic action to facilitate collagen I synthesis and its release, underscoring the enzymes' essential roles in skeletal health [39]. These enzymes contribute to the immediate repair mechanisms post-injury and influence bone remodeling and turnover by modulating ROS balance without affecting osteoclast viability [27]. This delicate equilibrium managed by MPO, and related enzymes ensures the prevention of excessive bone resorption by inhibiting osteoclast formation, thus playing a dual role in both the maintenance of bone health and the pathological progression of bone diseases where infiltrative immune cells introduce peroxidases to the bone environment [27]. Through these actions, peroxidase enzymes emerge as key players in the normal bone repair process and the complex interplay of factors governing bone pathology, offering new insights into their broader implications in bone health and disease management. In other words, ROS are pivotal in osteogenesis, stimulating osteoblasts while concurrently suppressing osteoclasts. The introduction of antioxidants,

however, dampens osteoblast activity and enhances osteoclast function, underscoring the crucial influence of ROS concentrations on skeletal development.

A deficit in NOX4, a crucial enzyme in ROS production, leads to diminished intracellular ROS. This decrease, attributed solely to the shortfall in the NOX4 enzyme among its family, ensures that the reduction in ROS does not reach detrimental levels. Such a deficit in NOX4 underscores its role in the nuanced modulation of intracellular ROS. While high ROS levels may precipitate cellular demise and disease, optimal ROS concentrations are vital for activating cellular signaling pathways essential for cellular endurance, equilibrium maintenance, and the aging response [33]. This delineates the critical nature of ROS modulation for skeletal health and genesis.

MPO plays a nuanced role in maintaining ROS balance during bone homeostasis and preserving bone integrity. Elevated MPO activity and other heme peroxidases facilitate osteoblast activation, markedly influencing bone development. The escalation in MPO, prompted by a NOX4-induced decrease in ROS, may directly affect bone formation processes, illustrating the intricate interplay between ROS generation, NOX4 activity, and MPO in skeletal biology.

OPN is widely recognized for its abundant presence in osteoblasts and mature osteoclasts, where it plays an essential role in various phases of bone structuring and formation. It's observed that an increase in ROS can dampen the Wnt/ β -catenin signaling pathway, a crucial conduit for promoting bone formation activities. Moreover, research has illuminated that a surge in β -catenin and RUNX2 expression correlates with heightened OPN levels, indicating osteoblast engagement [40]. This pattern intimates that a shortfall in NOX4, which is known to curtail ROS presence, might boost OPN expression by invigorating the Wnt/ β -catenin pathway. This interaction hints at a potential indirect linkage between NOX4 and OPN, underscoring their roles in bone health modulation. Therefore, it is pivotal to explore how NOX4, MPO, OPN, and their relationship with bone contribute to our understanding of skeletal health and development. A deficiency in NOX4 triggers a regulatory mechanism that adjusts intracellular ROS levels, subsequently influencing MPO and OPN expression. This modulation plays a vital role in bone formation and structure processes, which are essential for maintaining overall bone health.

In summary, our study compared the enhanced bone density and phenotype of bone formation in the femur of NOX4^{-/-} mice with that of normal mice and OVX mice. We observed an increase in the expression of inflammatory cytokines via proteome array, specifically MPO and OPN, in bone marrow-derived cells participating in bone formation in NOX4^{-/-} mice. While previous reports have suggested that the inhibition of NOX4 and the increased expression of MPO and OPN may enhance longitudinal growth for bone formation activity, this study is the first to provide evidence for the mechanistic connection between NOX4 and MPO or NOX4 and OPN in the context of bone function. Consequently, it is anticipated that the expression of MPO and OPN may depend on NOX4 expression-regulated mechanisms. MPO and OPN are expected to serve as excellent markers for bone formation alongside NOX4 and should be further investigated for their additional functions related to bone metabolism.

REFERENCES

1. Mackie EJ, Ahmed YA, Tatarczuch L, Chen KS, Mirams M. Endochondral ossification: how cartilage is converted into bone in the developing skeleton. *Int J Biochem Cell Biol.* 2008;40(1):46-62. [PUBMED](#) | [CROSSREF](#)
2. Ağirdil Y. The growth plate: a physiologic overview. *EFORT Open Rev.* 2020;5(8):498-507. [PUBMED](#) | [CROSSREF](#)
3. Bobick BE, Kulyk WM. Regulation of cartilage formation and maturation by mitogen-activated protein kinase signaling. *Birth Defects Res C Embryo Today.* 2008;84(2):131-154. [PUBMED](#) | [CROSSREF](#)
4. Schröder K. NADPH oxidases in bone homeostasis and osteoporosis. *Free Radic Biol Med.* 2019;132:67-72. [PUBMED](#) | [CROSSREF](#)
5. Joo JH, Huh JE, Lee JH, Park DR, Lee Y, Lee SG, et al. A novel pyrazole derivative protects from ovariectomy-induced osteoporosis through the inhibition of NADPH oxidase. *Sci Rep.* 2016;6(1):22389. [PUBMED](#) | [CROSSREF](#)
6. Cerqueni G, Scalzone A, Licini C, Gentile P, Mattioli-Belmonte M. Insights into oxidative stress in bone tissue and novel challenges for biomaterials. *Mater Sci Eng C.* 2021;130:112433. [PUBMED](#) | [CROSSREF](#)
7. Tao H, Ge G, Liang X, Zhang W, Sun H, Li M, et al. ROS signaling cascades: dual regulations for osteoclast and osteoblast. *Acta Biochim Biophys Sin (Shanghai).* 2020;52(10):1055-1062. [PUBMED](#) | [CROSSREF](#)
8. Bai Y, Gong X, Dou C, Cao Z, Dong S. Redox control of chondrocyte differentiation and chondrogenesis. *Free Radic Biol Med.* 2019;132:83-89. [PUBMED](#) | [CROSSREF](#)
9. Apel K, Hirt H. Reactive oxygen species: metabolism, oxidative stress, and signal transduction. *Annu Rev Plant Biol.* 2004;55(1):373-399. [PUBMED](#) | [CROSSREF](#)
10. Jomova K, Raptova R, Alomar SY, Alwasel SH, Nepovimova E, Kuca K, et al. Reactive oxygen species, toxicity, oxidative stress, and antioxidants: chronic diseases and aging. *Arch Toxicol.* 2023;97(10):2499-2574. [PUBMED](#) | [CROSSREF](#)
11. Pecchillo Cimmino T, Ammendola R, Cattaneo F, Esposito G. NOX dependent ROS generation and cell metabolism. *Int J Mol Sci.* 2023;24(3):2086. [PUBMED](#) | [CROSSREF](#)
12. Vermot A, Petit-Härtlein I, Smith SM, Fieschi F. NADPH oxidases (NOX): an overview from discovery, molecular mechanisms to physiology and pathology. *Antioxidants.* 2021;10(6):890. [PUBMED](#) | [CROSSREF](#)
13. Chen JR, Lazarenko OP, Blackburn ML, Chen JF, Randolph CE, Zabaleta J, et al. Nox4 expression in osteoprogenitors controls bone development in mice during early life. *Commun Biol.* 2022;5(1):583. [PUBMED](#) | [CROSSREF](#)
14. Goetsch C, Babelova A, Trummer O, Erben RG, Rauner M, Rammelt S, et al. NADPH oxidase 4 limits bone mass by promoting osteoclastogenesis. *J Clin Invest.* 2013;123(11):4731-4738. [PUBMED](#) | [CROSSREF](#)
15. Harrison C. Bone disorders: targeting NOX4 knocks down osteoporosis. *Nat Rev Drug Discov.* 2013;12(12):904-905. [PUBMED](#) | [CROSSREF](#)
16. Morel F, Rousset F, Vu Chuong Nguyen M, Trocme C, Grange L, Lardy B. NADPH oxidase Nox4, a putative therapeutic target in osteoarthritis. *Bull Acad Natl Med.* 2015;199(4-5):673-686. [PUBMED](#) | [CROSSREF](#)
17. Ambe K, Watanabe H, Takahashi S, Nakagawa T. Immunohistochemical localization of Nox1, Nox4 and Mn-SOD in mouse femur during endochondral ossification. *Tissue Cell.* 2014;46(6):433-438. [PUBMED](#) | [CROSSREF](#)
18. Long F, Ornitz DM. Development of the endochondral skeleton. *Cold Spring Harb Perspect Biol.* 2013;5(1):a008334. [PUBMED](#) | [CROSSREF](#)
19. Kozhemyakina E, Lassar AB, Zelzer E. A pathway to bone: signaling molecules and transcription factors involved in chondrocyte development and maturation. *Development.* 2015;142(5):817-831. [PUBMED](#) | [CROSSREF](#)
20. Berendsen AD, Olsen BR. Bone development. *Bone.* 2015;80:14-18. [PUBMED](#) | [CROSSREF](#)
21. Tobeiha M, Moghadasian MH, Amin N, Jafarnejad S. RANKL/RANK/OPG pathway: a mechanism involved in exercise-induced bone remodeling. *BioMed Res Int.* 2020;2020:6910312. [PUBMED](#) | [CROSSREF](#)
22. Datta HK, Ng WF, Walker JA, Tuck SP, Varanasi SS. The cell biology of bone metabolism. *J Clin Pathol.* 2008;61(5):577-587. [PUBMED](#) | [CROSSREF](#)
23. Franz-Odenaal TA. Induction and patterning of intramembranous bone. *Front Biosci (Landmark Ed).* 2011;16(7):2734-2746. [PUBMED](#) | [CROSSREF](#)
24. Galea GL, Zein MR, Allen S, Francis-West P. Making and shaping endochondral and intramembranous bones. *Dev Dyn.* 2021;250(3):414-449. [PUBMED](#) | [CROSSREF](#)

25. Safadi FF, Barbe MF, Abdelmagid SM, Rico MC, Aswad RA, Litvin J, et al. Bone structure, development and bone biology. In: Khurana JS, editor. *Bone Pathology*. Humana Totowa: Humana Press; 2009, 1-50.
26. Chen JR, Lazarenko OP, Zhao H, Wankhade UD, Pedersen K, Watt J, et al. Nox4 expression is not required for OVX-induced osteoblast senescence and bone loss in mice. *JBMR Plus*. 2020;4(8):e10376. [PUBMED](#) | [CROSSREF](#)
27. Zhao X, Lin S, Li H, Si S, Wang Z. Myeloperoxidase controls bone turnover by suppressing osteoclast differentiation through modulating reactive oxygen species level. *J Bone Miner Res*. 2021;36(3):591-603. [PUBMED](#) | [CROSSREF](#)
28. Ishijima M, Rittling SR, Yamashita T, Tsuji K, Kurosawa H, Nifuji A, et al. Enhancement of osteoclastic bone resorption and suppression of osteoblastic bone formation in response to reduced mechanical stress do not occur in the absence of osteopontin. *J Exp Med*. 2001;193(3):399-404. [PUBMED](#) | [CROSSREF](#)
29. Si J, Wang C, Zhang D, Wang B, Zhou Y. Osteopontin in bone metabolism and bone diseases. *Med Sci Monit*. 2020;26:e919159. [PUBMED](#) | [CROSSREF](#)
30. Chen J, Singh K, Mukherjee BB, Sodek J. Developmental expression of osteopontin (OPN) mRNA in rat tissues: evidence for a role for OPN in bone formation and resorption. *Matrix*. 1993;13(2):113-123. [PUBMED](#) | [CROSSREF](#)
31. Khan AA, Alsahli MA, Rahmani AH. Myeloperoxidase as an active disease biomarker: recent biochemical and pathological perspectives. *Med Sci (Basel)*. 2018;6(2):33. [PUBMED](#) | [CROSSREF](#)
32. Boonpraman N, Yoon S, Kim CY, Moon JS, Yi SS. NOX4 as a critical effector mediating neuroinflammatory cytokines, myeloperoxidase and osteopontin, specifically in astrocytes in the hippocampus in Parkinson's disease. *Redox Biol*. 2023;62:102698. [PUBMED](#) | [CROSSREF](#)
33. Checa J, Aran JM. Reactive oxygen species: drivers of physiological and pathological processes. *J Inflamm Res*. 2020;13:1057-1073. [PUBMED](#) | [CROSSREF](#)
34. Hajam YA, Rani R, Ganie SY, Sheikh TA, Javaid D, Qadri SS, et al. Oxidative stress in human pathology and aging: molecular mechanisms and perspectives. *Cells*. 2022;11(3):552. [PUBMED](#) | [CROSSREF](#)
35. Del Valle LG. Oxidative stress in aging: theoretical outcomes and clinical evidences in humans. *Biomed Aging Pathol*. 2011;1(1):1-7. [CROSSREF](#)
36. DeNichilo MO, Shoubridge AJ, Panagopoulos V, Liapis V, Zysk A, Zinonos I, et al. Peroxidase enzymes regulate collagen biosynthesis and matrix mineralization by cultured human osteoblasts. *Calcif Tissue Int*. 2016;98(3):294-305. [PUBMED](#) | [CROSSREF](#)
37. Ramp WK, Arnold RR, Russell JE, Yancey JM. Hydrogen peroxide inhibits glucose metabolism and collagen synthesis in bone. *J Periodontol*. 1987;58(5):340-344. [PUBMED](#) | [CROSSREF](#)
38. Baldus S, Eiserich JP, Mani A, Castro L, Figueroa M, Chumley P, et al. Endothelial transcytosis of myeloperoxidase confers specificity to vascular ECM proteins as targets of tyrosine nitration. *J Clin Invest*. 2001;108(12):1759-1770. [PUBMED](#) | [CROSSREF](#)
39. Cox G, Einhorn TA, Tzioupis C, Giannoudis PV. Bone-turnover markers in fracture healing. *J Bone Joint Surg Br*. 2010;92(3):329-334. [PUBMED](#) | [CROSSREF](#)
40. Atashi F, Modarressi A, Pepper MS. The role of reactive oxygen species in mesenchymal stem cell adipogenic and osteogenic differentiation: a review. *Stem Cells Dev*. 2015;24(10):1150-1163. [PUBMED](#) | [CROSSREF](#)